

Performance Evaluation of Industrial Air-Shower in Removal of Gas- and Liquid-Phase Contaminants from Human Body

Li, Cong

Interdisciplinary Graduate School of Engineering Sciences, Kyushu University

Ito, Kazuhide

Interdisciplinary Graduate School of Engineering Sciences, Kyushu University

<https://doi.org/10.5109/1440976>

出版情報 : Evergreen. 1 (1), pp.40-47, 2014-03. Green Asia Education Center
バージョン :
権利関係 : Creative Commons Attribution-NonCommercial 4.0 International

Performance Evaluation of Industrial Air-Shower in Removal of Gas- and Liquid-Phase Contaminants from Human Body

Cong Li, Kazuhide Ito^{*}

Interdisciplinary Graduate School of Engineering Sciences, Kyushu University

^{*}Author to whom correspondence should be addressed, Email: ito@kyudai.jp

(Received February 18, 2014; accepted February 28, 2014)

In scenarios of terrorist strikes or severe disasters involving the dispersion of nuclear, biological, or chemical pollutants, rapid and effective decontamination and removal of such contaminants from the human body become critically important tasks during rescue operations. Because of the limitations of the globally used wet and dry decontamination processes from the viewpoints of processing speed and large size of the device required, this study developed a wind decontamination system in which forced convective flow is applied against the human body surface, similar to an industrial air-shower system. This study evaluated the decontamination performance of a prototype air-shower system with the aim of verifying the industrial feasibility of the wind decontamination system. Fundamental experiments were conducted to investigate the contaminant removal efficiency of the air-shower system by using hypothetical liquid-phase (pure liquid water) and gas-phase (SF₆ gas) contaminants. The results revealed that the removal efficiency for the gas-phase contaminant could exceed 90% within a 30-s purging time duration in the decontamination process. A corresponding CFD simulation of the experimental setup was also carried out, and the contribution ratio of each air supply inlet opening of the air-shower system was discussed.

1. Introduction

Following a severe accident, disaster, or intentional release/dispersion of nuclear, biological, or chemical (NBC) pollutants in a terrorist strike, indoor residents are at severe risk of being exposed to hazardous contaminants. When a disaster occurs and an individual is exposed to hazardous contaminants, prompt action for reducing the exposure risk, i.e., decontamination, is an indispensable task (Binder S, 1989). The aim of decontamination is to rapidly and effectively remove the hazardous pollutants from the human body and to thus reduce health risk. Basic methods of decontamination include physical removal and chemical or biological deactivation of agents (Okumura T, 1998; Bronstein AC and Currance PL, 1994). Chemical agents can be washed and rinsed away with water or aqueous solutions; alternatively, they can be dried up or removed by heat treatment (Brockman JE, 1998; Kumar V, et al., 2010; Favata EA and Gochfeld M, 1990). Generally, the first two methods, which are called wet and dry decontamination, respectively, are regarded as global and basic countermeasures, especially in a scenario of chemical accidents caused by gas- and liquid-phase contaminants. However, both these methods have certain limitations. Decontamination using water has varied advantages, but in the application of this method, it is difficult to provide privacy to victims during the

decontamination process and to set up the device quickly.

In case of hundreds of victims exposed to hazardous contaminants in a disaster scenario, an effective and rapid decontamination method needs to be developed to be able to respond rapidly while also subsiding the feeling of panic among the victims.

The primary objective of this study is to develop a new and alternative decontamination procedure using forced convective flow, i.e., a wind decontamination system (hereafter referred to as WDCS). As the name implies, a WDCS works on the principle of applying forced convective flow to the human body surface to increase the mass transfer of the contaminant, thereby enhancing the desorption or detachment of the contaminant from the human body; this principle is similar to that of an industrial air-shower system. We have previously conducted wind tunnel experiments and investigated the convective heat transfer coefficients of the human body under strong convective wind conditions as first approximations to the controlling parameters of the heat and mass transfer from the skin surface (Li C, et al., 2012). Now, the aim of the present study is to verify the decontamination performance of the developed WDCS by adopting an industrial air-shower system as the prototype model.

Although industrial air-shower systems are widely adopted in industrial factories and clean rooms, a performance evaluation method and index of

decontamination efficiency of these systems have not yet been well discussed; therefore, development of qualitative and quantitative evaluation methods is necessary. In general, the design method of industrial air-shower system is kept open-ended; and the guidebook written by Austin PR (1970), however, is one of the few exceptions. The information in this guidebook, though useful, is relatively outdated and should hence be updated by conducting detailed experiments and numerical simulations. Then, an overarching purpose of this study is to provide fundamental data on a design of a general industrial air-shower system.

2. WDCS based on industrial air-shower system

In this study, we developed a prototype model of the WDCS, which is based on an industrial air-shower system. Figure 1 (1) shows a photograph of the developed prototype of the WDCS. The WDCS is developed for use on one individual at a time, and the dimensions of the inner treatment (purging) space are 0.8 m (X) × 0.82 m (Y) × 1.81 m (Z). The entry and exit doors are designed for rapid, one-way handling for in-order treatment of large numbers of victims.

A large-sized circular nozzle with a diameter of 15.1 cm is fixed on the ceiling as the main supply inlet and is used for generating a uniform vertical flow from top to bottom in order to prevent recirculation of the contaminant, especially in the breathing zone. Nine small-sized nozzles (Punkah Louver) are installed on the left and right walls to ensure the purging of the contaminant from the local dead zone of the human body, e.g., the axilla and the inner side of legs. The supply and exhaust airflows are controlled by a total of four blowers (two each are used for supply and exhaust, 1.5 kW), and the flow rate and indoor pressure can be precisely controlled sequentially by inverter control, as shown in Figure 1 (2). Referred to Austin PR (1970), particles deposited on a surface can be efficiently removed at a critical velocity of 18 m/s within a removal time of 10 s. For our prototype air-shower system, the total airflow rate was kept constant at 54.3 m³/min (33.5 ACM) and under this condition, the maximum inlet air velocity could increase to more than 30 m/s in the vicinity of the supply inlet (which is fixed on the ceiling).

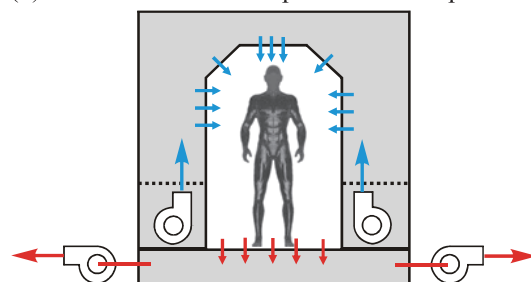
3. Experiment estimation of removal efficiency of air-shower system

3.1 Outline of experiment 1 (Liquid-phase contaminant)

In the initial stage of this study, pure liquid water was used as a hypothetical liquid-phase contaminant. In general, removal of a liquid-phase contaminant adsorbed inside clothing is more difficult than that of a gas-phase contaminant because of the diffusion resistance inside clothing.



(1) Exterior and interior spaces of developed WDCS



(2) Outline of airflow in air-shower system





Fig. 1 Industrial air-shower system.

From this viewpoint, an experiment performed with a liquid-phase contaminant absorbed inside clothing could provide data for evaluating the critical performance of an air-shower system in terms of the contaminant removal efficiency. In other words, the case of using pure water as a substitute for a liquid-phase contaminant could elucidate the potential removal efficiency of the air-shower system for various types of contaminants.

In this experiment, manikins having proportions of a human child and adult were used as virtual human bodies. In addition, two cylindrical models (SUS, $\Phi=0.3$ m) with surface areas equal to those of the child and adult manikins were adopted to investigate the influence of human geometry on the contaminant removal efficiency. The manikins were clothed in summer or winter clothing for evaluating the impact of the clothing volume (i.e., extent). Furthermore, a pure cotton bandage was used to represent basic clothing material for both the manikins and the cylindrical models, as specified in Table 1. The direction of wind approaching the human body is expected to have a definite impact on the contaminant removal efficiency for each body segment. Therefore, two different wind directions were set by adjusting the standing position of the experimental manikin: cross-wind direction and facing wind direction. Since the total air flow rate and average velocity of supply inlets are extremely high, it is believable that the temperature and humidity of the inlet air have comparatively very little effect on the removal efficiency of the WDCS. During the experiment, the temperature and relative humidity of the supply air were not precisely controlled but instead maintained at approximately $15\text{ }^{\circ}\text{C} \pm 3\text{ }^{\circ}\text{C}$ and $40\% \pm 15\%$, respectively.

Optimization of the purging time duration is important in the application of the air-shower system for

Table 1 Experimental subjects and clothing ensembles.

Experimental subject	Child cylinder	Child manikin	Adult cylinder	Adult manikin
				
Height	0.68 m	1.20 m	1.60 m	1.82 m
Body area	0.71 m ²	0.71 m ²	1.59 m ²	1.59 m ²
Bandage	4 layers	4 layers	4 layers	4 layers
Summer-wear ensemble	—	T-shirt; briefs; shorts; socks	—	briefs; short-sleeved shirt; suit trousers; tie; belt; socks
Winter-wear ensemble	—	undershirt; briefs; sweater (×2); jeans; socks	—	undershirt; briefs; shirt; tie; belt; socks

decontamination. In this experiment, four time durations were considered: 10, 30, 60, and 180 s. As the initial condition for exposing the experimental subject to the contaminant, a total of 50 g of pure liquid water was uniformly sprayed on the surface of the manikins' clothing, and subsequently, an exposure time of 10 min was assumed to be reasonable sufficient for the water diffusion inside the clothing. The pre-wet experimental manikin was then subjected to purging treatment inside the air-shower system, where the total weight change of the manikin before and after the treatment ($m_1 - m_2$) was measured using a precise electric balance (A&D, GP-30KS, with accuracy of 0.1 g). According to the same experimental procedure, each experimental case was investigated repeatedly at least five times. The results of the experiment were indicated as an ensemble averaged value.

The removal efficiency η_{liquid} [%] is defined as in Equation (1):

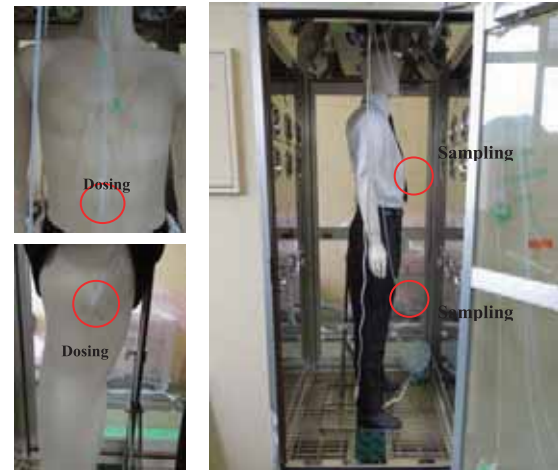
$$\eta_{liquid} = \left(\frac{m_1 - m_2}{m_1} \right) \times 100 \quad (1)$$

Here, m_1 [g] and m_2 [g] respectively denote the water amount inside the clothing before and after the purging treatment.

3.2 Outline of experiment 2 (Gas-phase contaminant)

Gas-phase contaminants are considered as some of the most dominant contaminants in NBC terrorism and play an important role in short- and long-term exposures in indoor environments. SF₆ gas, having a molar weight identical to Sarin (a toxic industrial chemical and harmful contaminant used in terrorist attacks), was used as a hypothetical gas-phase contaminant in this study.

Prior to the gas-phase experiment, the air-tightness of the inner space of the air-shower system was measured under the "off" condition of all the blowers. All of the supply inlets were well sealed. Two dosing points of SF₆

**Fig. 2** Experiment setup in case of gas-phase contaminant.

gas were set on the inner side of the clothing, and two sampling points were set in the inner space of the air-shower system, as shown in Figure 2. These dosing and sampling points were connected to the concentration measurement instrument (INNOVA multi-gas monitor) to control the initial injection amount of SF₆ and to monitor the concentration decay after the purging treatment. SF₆ is an inert gas, and therefore, when it transfers through clothing, its adsorption on wall surfaces (wall surface material: SUS 304) inside the air-shower system is assumed to be negligible. After sufficient time elapsed for diffusion or dispersion to occur, the concentration of SF₆ gas inside the air-shower system achieved a steady state and that was considered to be a representative concentration, i.e., an equilibrium concentration.

The equilibrium concentration is an important value in calculating the removal efficiency of WDACS in case of gas-phase contaminant. It should be measured at two stages: after initial contamination, c_1 [ppm], and during post-purging operation, c_2 [ppm].

The gas-phase removal performance η_{gas} [%] of the air-shower system is quantitatively evaluated by obtaining the difference in the gas concentrations before and after the purging treatment, as expressed in Equation (2):

$$\eta_{gas} = \left(\frac{c_1 - c_2}{c_1} \right) \times 100 \quad (2)$$

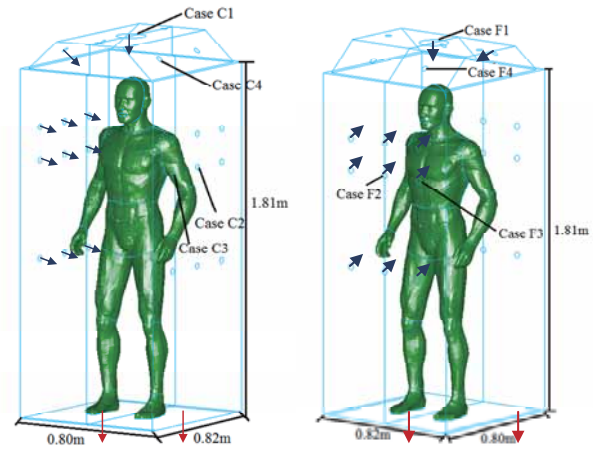
Owing to the complexity in the processing of a gas-phase contaminant, only adult manikins were employed in the gas-phase experiment and three purging time durations—10, 30, and 60 s—were selected under the cross-wind and facing wind directions. Each case was repeated at least five times and the average value was used in the calculation of removal efficiency. The boundary conditions including, but not limited to, airflow, temperature, and relative humidity were kept identical to those in the liquid-phase contaminant experiments.

4. CFD simulation of contribution ratio of each supply inlet

For further investigation of the developed WDCS, a corresponding CFD simulation was performed, and the contribution ratio of each supply inlet of the above-described experimental air-shower system was discussed. The CFD simulation reproduced the dimensions of the air-shower system and integrated a virtual manikin into the analytical domain, as shown in Figure 3.

The virtual manikin (standing male-proportioned human model) was reproduced to some extent with detailed geometries of body parts such as ears, nose, fingers, and toes. This virtual manikin imitated the average Japanese male body proportions. The outlines of the human body were drawn using POSER 4.0J software (Curious Labs Inc.), and the data was then read-out in DXF format. The overall shape of the human body was then adjusted using three-dimensional (3D) CAD software (Vector Works and A&A Co., Ltd.). The final geometries of the virtual manikin and computational grids were generated using the commercial mesh generator GRIDGEN V15 software (VINAS Co., Ltd.). The hands and feet of the virtual manikin were simplified in consideration of the computational load for the CFD analysis. Detailed information on the virtual manikin developed by our group is provided elsewhere (Ito K and Hotta T, 2006). To establish the boundary layer around the virtual manikin, prism cells were created at the surface and dimensionless length y^+ was kept to 1.0 or less. The tetra meshes were then arranged from the outside of the boundary layer to the other side walls in the analytical domain.

The flow field and mass transfer of the inner space in the air-shower system were analyzed three-dimensionally by using commercial CFD code ANSYS/FLUENT 12.1 (ANSYS, 2009). SST $k-\omega$ model was employed in CFD simulation and conducted steady-state calculation. The



(1) Cross wind

(2) Facing wind

Fig. 3 Analytical domain of air-shower system.

SIMPLE algorithm was used with the second-order upwind scheme for the convective terms, and a second-order central difference scheme was used for the other terms. The no-slip condition was adopted as the wall surface boundary condition for velocity. In this analysis, isothermal conditions were assumed. The numerical boundary conditions were the same as those in the air-shower experiment, as listed in Table 2.

After the flow field analysis, the contribution ratio was analyzed using the concept of SVE4 (i.e., the scale for ventilation efficiency, No. 4) proposed by Kato S and Yang J (Kato S and Yang J, 2008). SVE4 is defined as follows:

$$SVE4(X, n) = C_X(X, n) / C_0(n) \quad (3)$$

$$C_0(n) = q / Q(n) \quad (4)$$

where $SEV4(X, n)$ is the contribution ratio of the n th supply opening at point X . C_X denotes the contribution of the tracer at the n th supply opening; C_0 is the concentration under a perfect mixing condition and is expressed using the tracer generation rate q [kg/s] and total airflow rate Q [m³/s] at the n th supply opening.

In the numerical simulation, a hypothetical scalar ϕ that represents the passive contaminant transported by the n th air supply opening was defined, and the contribution ratio could be estimated straightforwardly. The user-defined scalar transport equation in ANSYS/FLUENT is as follows:

$$\frac{\partial \rho \phi_k}{\partial t} + \frac{\partial}{\partial x_i} (\rho u_i \phi_k - \Gamma_k \frac{\partial \phi_k}{\partial x_i}) = S_{\phi_k} \quad (5)$$

Here, Γ_k and S_{ϕ_k} denote the diffusion coefficient and source term, respectively, for the k th user-defined scalar.

Different cases corresponding to different wind supply inlets in the SVE4 calculation were analyzed, as listed in Table 3; these cases are marked in Figure 3.

Table 2 Numerical boundary conditions for CFD simulation of air-shower system.

Turbulence model	SST $k-\omega$ model (3D calculation)
Scheme	Convective term: QUICK
Inflow boundary	Diameter of main inlet: 15.1 cm
	Diameter of supplementary inlet: 3.2 cm
	$U_{in} = 24.3$ m/s, $TI = 5\%$, $k_{in} = 3/2 \times (U_{in} \times TI)^2$,
	$\varepsilon_{in} = C_{\mu} \times k_{in}^{3/2}/l_{in}$, $C_{\mu} = 0.09$, $l_{in} = 0.03$ m
Inflow direction	Normal direction to wall
Outflow boundary	$U_{out} = \text{Free slip}$, $k_{out} = \text{Free slip}$, $\varepsilon_{out} = \text{Free slip}$
Wall treatment	Velocity: No slip, $k _{wall}$: No slip
Surface treatment of human model	Velocity: No slip, $k _{wall}$: No slip

Table 3 Analytical cases in CFD simulation of air-shower system.

Analytical case (see Figure 2)	Relative position of human model against side wall	Supply slot angle
Case C1	Cross wind	Normal to the wall
Case C2		
Case C3		
Case C4		
Case F1	Facing wind	
Case F2		
Case F3		
Case F4		

5. Results and discussion

5.1 Removal efficiency of air-shower system

The removal efficiency η in the case of liquid-phase contaminant as a function of purging time duration for adult cases is shown in Figure 4. The η values were highly dependent on the decontamination time. In the context of the body shape and extent of clothing, the cylindrical model having a simple geometry with cotton bandage achieved a relatively lower η than the other experimental cases with complicated body geometries and multilayered garments.

The lowest value of η was observed for the manikin dressed in winter clothes. From the viewpoints of water diffusion and adsorption inside the clothing, a low removal efficiency indicated the occurrence of a complex diffusion process inside the composite winter garments, which are multilayered and made primarily of polyester. In addition, the child manikin showed lower removal efficiency than the adult manikin because the main supply jet on the ceiling could not efficiently aim at and reach the child manikin, owing to its smaller height than the adult manikin, as shown in Figure 5.

As expected, the removal efficiency in the gas-phase experiment was much higher than that in the liquid-phase experiment, and it could exceed 90%, as shown in Figure 6. The effect of extent of clothing on the change in η was similar to the corresponding results obtained in the liquid-phase experiment.

From the experimental results, it was also confirmed that the standing direction and position of the manikin affected the decontamination efficiency. In general, when

the subjects were in the cross-wind position, a large amount of airflow supplied from the left and right walls was parallel to the clothing on the front and back sides of the subject. On the contrary, a direct flow impinging onto a facing-wind-positioned subject supplied from the left and right walls increased the mass transfer efficiency. Hence, a relatively superior performance was observed in the facing wind position for both the liquid-phase and the gas-phase experiments.

We also tested another type of air-shower system, whose photograph and details experimental results are presented in Appendix. Specifically, the Appendix briefly presents the removal efficiency results for this system. The difference between the removal efficiencies of these two air-shower systems may be attributed to the differences in the inlet airflow rate and also the differences in the inlet air velocity.

5.2 Contribution ratio of supply inlets

Figure 7 (1) shows three views of the field distribution around the virtual manikin in the cross-wind direction. This figure shows that a uniform flow field was generated around the human model from the top to the bottom throughout the analytical domain.

A symmetric flow field centered around the human model was confirmed. The main supply inlet on the ceiling is closer to the head of the model than are the supplementary inlets on the walls; therefore, the main supply inlet has a strong effect on the head. The flow ejected toward the chest and back originated mainly from the supplementary openings on the walls. In addition, a symmetric flow field centered around the human model

was generated.

Figure 7 (2) shows three views of the flow field distribution around the virtual manikin in the facing wind direction. Similar to the cross-wind direction, in the facing wind direction as well, the flow originating from the main supply on the ceiling was ejected with a heavy force on the head. Specially, this flow had a larger contribution to the chest and back of the human model as compared to that in the cross-wind direction. Then, the flows from the main supply inlet and from the supplementary inlets mixed in the bottom half of the WDCS room.

Figure 8 shows the contours of SVE4 around the virtual manikin for different cases, i.e., C1–F4, numbered according to the supply source.

For Case C1, the target scalar in the SVE4 calculation was supplied from the ceiling, and the calculated SVE4 values at the head and chest in this case were 72.2% and 50%, respectively. Note that in the CFD analysis, the considered inlet velocity was an average value; in other words, the main supply inlet on the ceiling accounted for 48.1% of the total airflow rate. Given this, the main supply inlet had a much larger contribution than did the other supplementary openings.

In case C2, i.e., the scalar in SVE4 calculation supplied from the center nozzle on the wall, the obtained SVE4 value was 10.5% on the left arm and 4.6% on the left side of the head. The target nozzle in Case C3 was oriented parallel to that in Case C2, and in this case the maximum SVE4 (8.2%) was observed on the front side of the shoulder. This value is 22% lower than that in Case C2. For the final case in the cross-wind direction, i.e., Case C4, the scalar supplied from one of the supplementary inlets on the ceiling, and the SVE4 value in this case was 10% on the left side of the head.

Figure 8 (2) shows the SVE4 distributions in the facing wind direction. The distribution pattern for case F1 was the same as that for Case C1. However, with three nozzles normally ejecting flow toward the chest (Case F2), a maximum SVE4 value of 6.7% was obtained at the chest. This value is relatively smaller than those in the other cases in the facing wind direction (Cases F1, F3 and F4). This behavior can be explained by the fact that, as seen in Figure 7 (2a), the flow from the main supply inlet on the ceiling covered the surface of the entire body but prevented the flow impinging normally on the chest. In other words, a large flow from the top (ceiling) blocked the flow directed normally toward the chest. This is the reason for the estimated SVE4 value in Case F2 being smaller than Case F1, F3 and F4.

6. Conclusion

This study was aimed at evaluating the industrial applicability of a developed wind decontamination system (WDCS) during response to emergency accidents in which humans may be exposed to hazardous biological

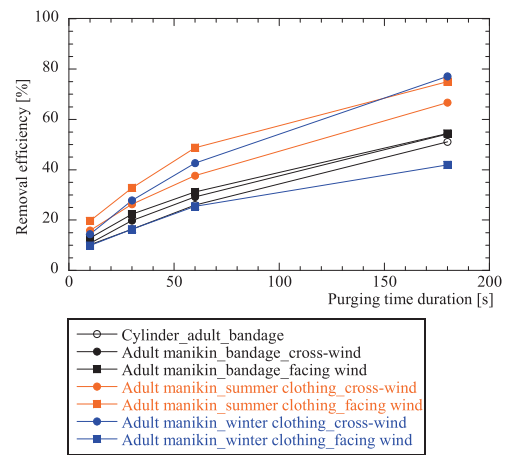


Fig. 4 Contaminant removal efficiency as a function of purging time duration for adult models in liquid-phase experiment.

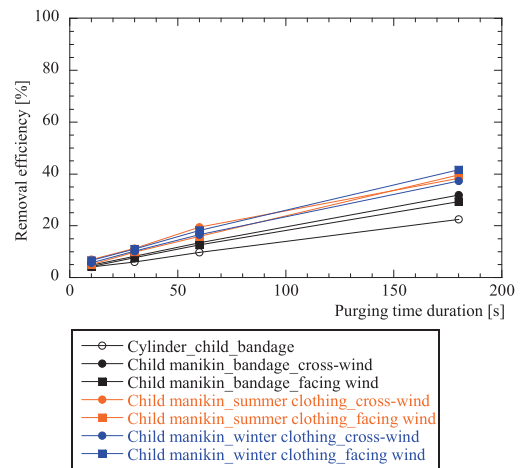


Fig. 5 Contaminant removal efficiency as a function of purging time duration for child models in liquid-phase experiment.

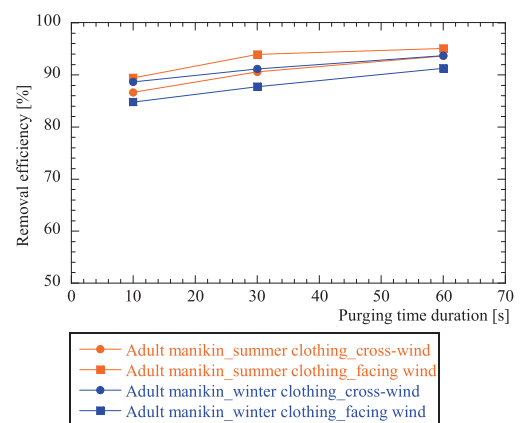


Fig. 6 Contaminant removal efficiency as a function of purging time duration for adult models in gas-phase experiment.

or chemical contaminants. An industrial air-shower system was used as a prototype model of the WDCS; the system was used for investigating the removal efficiency of the WDCS through fundamental experiments in which

pure water was used as the liquid-phase contaminant and SF₆ gas was used as the gas-phase contaminant.

The experimental findings showed that under the considered experimental conditions, the maximum removal efficiency achieved was approximately 80% in the case of a liquid-phase contaminant (for a purging time duration of 180 s) and more than 90% in the case of a gas-phase contaminant (for a purging time duration of 60 s). These high removal efficiencies of the air-shower system confirmed the feasibility of industrial application of the WDCS. Furthermore, the results of the fundamental experiments also confirmed that the removal efficiency of the air-shower system was strongly dependent on the purging time duration, the types (i.e., extent) of clothing, and the size and geometry of the human model used in the experiment.

For investigating the WDCS further, a numerical simulation was conducted that estimated the contribution ratio SVE4 of each supply inlet. The simulation results revealed that the main supply on the ceiling contributed a considerably large quantity of SVE4 to the upper part of the human body. The SVE4 value was more than 50% on the chest and over 70% on the head. However, for the supplementary openings, the maximum contribution ratio was only 10%. One of the reasons for this result is that the large amount flow from the top, i.e., ceiling, blocked the flow ejected from the supplementary openings.

It should however be noted that some uncertainties existed while conducting the experiments, e.g., the control of boundary conditions and experiment reproducibility. To optimize and maximize the removal efficiency of the WDCS, further studies are required, which would be specifically targeted at exploring its industrial applicability.

Appendix

Various types of air-shower systems are commercially used in the food and semiconductor industries. These systems have their own customized supply inlet slots, wind directions, and airflow rate. Here, we present the performance evaluation results for a commercially used air-shower system that is different from the WDCS.

Figure A1 shows photographs of the inner space of the industrial air-shower system that is commercially used in Japan. This system has a total of 21 nozzles of the same size, out of which eight nozzles each are installed on the left and right walls and five nozzles are installed on the ceiling. We evaluated the removal efficiency of this system by conducting a liquid-phase experiment using pure liquid water as a hypothetical liquid-phase contaminant. Note that the airflow rate of this system is 25 m³/min, which is nearly half that of the air-shower system considered in the main study. The inlet air velocity of the commercial system is also lower - approximately 18 m/s in the vicinity of each supply inlet. These parameters may have resulted in the relatively lower removal efficiency of this commercial system. As

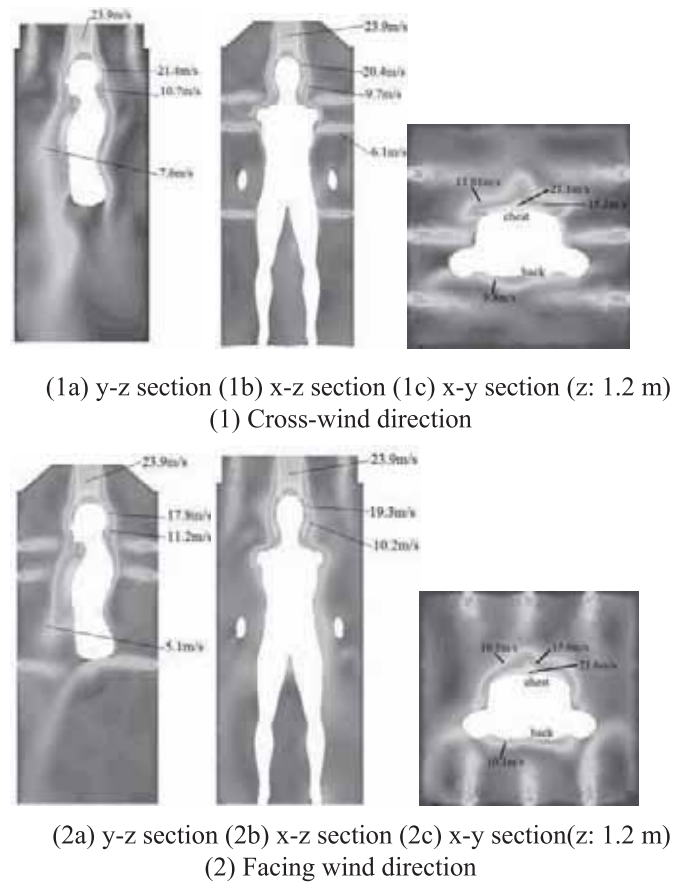


Fig. 7 Flow field distributions [m/s].

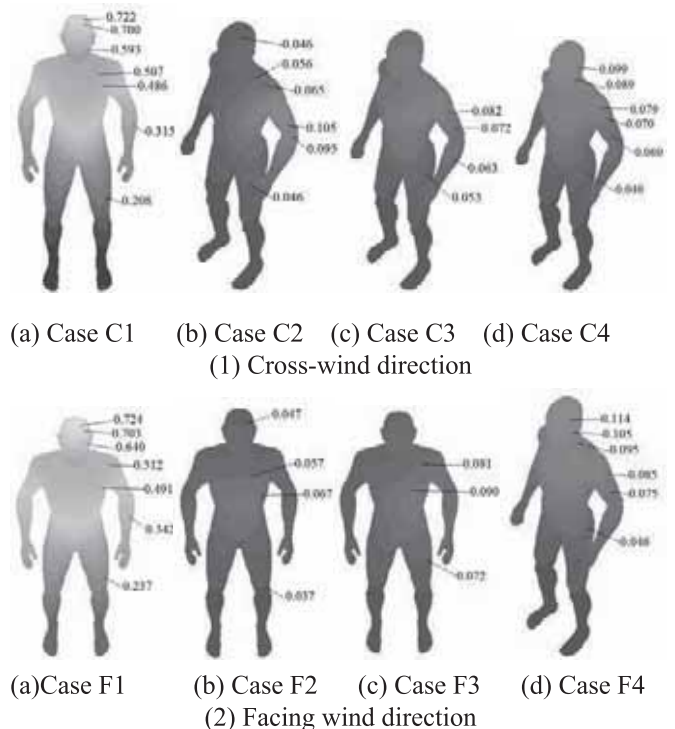


Fig. 8 SVE4 distributions in two wind directions.

is clear from Figure A2, the removal efficiency of this system is much lower than that of the main system used in the study, especially in the case of adult models.

Acknowledgement

This project was partially supported by a grant from the Fire and Disaster Management Agency of the Ministry of Internal Affairs and Communication in Japan and partially by a Grant-in-Aid for Scientific Research (JSPS KAKENHI for Young Scientists (S), 21676005). The authors would like to express special thanks to these funding sources.

References

- 1) ANSYS Fluent 12.1 Theory Guide (2009).
- 2) P. R. Austin, *Design and operation of clean rooms*, Business News Pub. Co., Detroit (1970).
- 3) S. Binder, *Am. J. Public Health* **79**, 1042-1044 (1989).
- 4) A. C. Bronstein, P. L. Currance, 1994. *Emergency care for hazardous materials exposure*, Second ed., Mosby Lifeline St. Louis (1994).
- 5) J. E. Brockman, *Removal of sarin aerosol and vapor by water sprays*, Sandia National Laboratories, Albuquerque, (1998).
- 6) E. A. Favata, M. Gochfeld, *Occup. Environ. Med.*, **5**, 79-91 (1990).
- 7) K. Ito, T. Hotta, *Transactions of SHASE (The Society of Heating, Air-Conditioning and Sanitary Engineers of Japan)*, **113**, 27-34 (2006). (In Japanese)
- 8) S. Kato, J. Yang, *Build Environ.* **43**, 494-507 (2008).
- 9) V. Kumar, R. Goel, R. Chawla, M. Silambarasan, R. K. Sharma, *J. Pharm. Bioallied Sci.*, **2**, 220-238 (2010).
- 10) C. Li, E. Lim, K. Ito, *Transactions of SHASE (Society of Heating, Air-conditioning and Sanitary Engineers of Japan)*, **183**, 47-57 (2012). (In Japanese)
- 11) T. Okumura, K. Suzuki, A. Fukuda, A. Kohama, N. Takasu, S. Ishimatsu, S. Hinohara, *Acad. Emerg. Med.*, **5**, 618-624 (1998).
- 12) T. Okumura, K. Suzuki, A. Fukuda, A. Kohama, N. Takasu, S. Ishimatsu, S. Hinohara, *Acad. Emerg. Med.*, **5**, 625-628 (1998).



Fig. A1 Photographs of inner space of air-shower system used commercially in Japan.

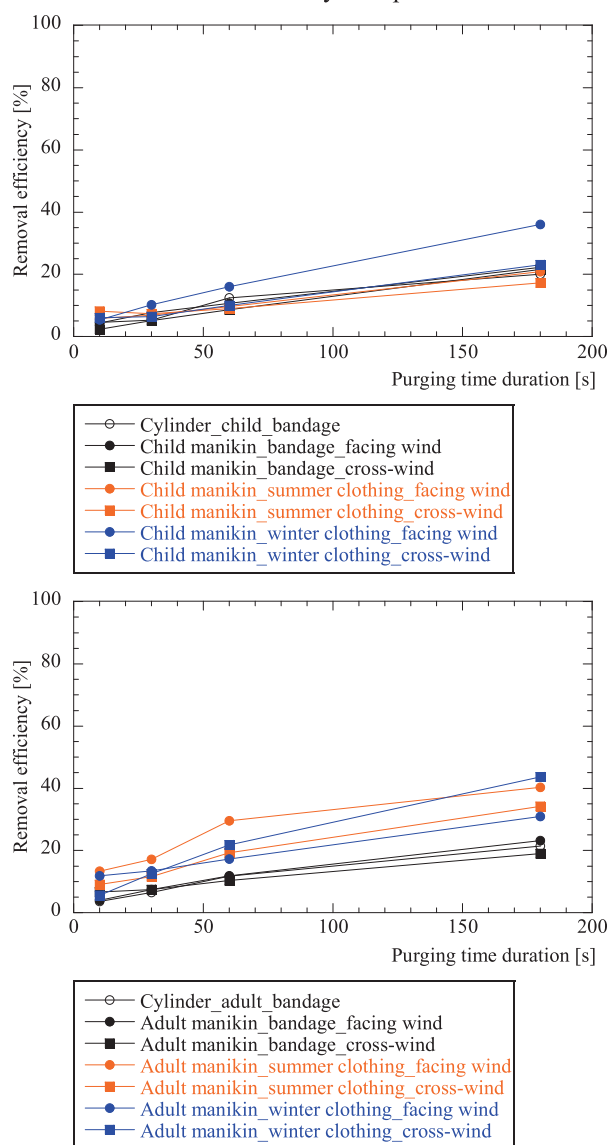


Fig. A2 Removal efficiency of commercial system in liquid-phase experiment.